Chinese Chemical Letters 35 (2024) 109103

Contents lists available at ScienceDirect

Chinese Chemical Letters

journal homepage: www.elsevier.com/locate/cclet

Simple-structured hydrophilic sensors for sweat uric acid detection with laser-engraved polyimide electrodes and cellulose paper substrates

Linhe Xu[a,1], Xueshan Hu[b,1], Shuang Zhou[a], Ze Zhang[a], Junxian Zhang[a], Chao Li[b], Daxian Zuo[b], Hao Liu[a], Gang Chen[a], Jiayu Wan[b,*], Jinsong Tao[a,*]

[a] State Key Lab of Pulp and Paper Engineering, South China University of Technology, Guangzhou 510640, China
[b] Future Battery Research Center, Global Institute of Future Technology, Shanghai Jiao Tong University, Shanghai 200240, China

ARTICLE INFO

Article history:
Received 31 July 2023
Revised 25 August 2023
Accepted 14 September 2023
Available online 16 September 2023

Keywords:
Laser-engraved carbon
Polyimide
Cellulose paper
Hydrophilicity
Sweat uric acid

ABSTRACT

Accurate detection of uric acid (UA) is crucial for diagnosing gout, yet traditional sweat-based UA sensors continue to face challenges posed by complex and costly electrode fabrication methods, as well as weakly hydrophilic substrates. Here, we designed and developed simple, low-cost, and hydrophilic sweat UA detection sensors constructed by carbon electrodes and cellulose paper substrates. The carbon electrodes were made by carbonized polyimide films through a simple, one-step laser engraving method. Our electrodes are porous, possess a large specific surface area, and are flexible and conductive. The substrates were composed of highly hydrophilic cellulose paper that can effectively collect, store, and transport sweat. The constructed electrodes demonstrate high sensitivity of 0.4 μA L μmol^{-1} cm^{-2}, wide linear range of 2–100 μmol/L. In addition, our electrodes demonstrate high selectivity, excellent reproducibility, high flexibility, and outstanding stability against mechanical bending, temperature variations, and extended storage periods. Furthermore, our sensors have been proven to provide reliable results when detecting UA levels in real sweat and on real human skin. We envision that these sensors hold enormous potential for use in the prognosis, diagnosis, and treatment of gout.

© 2024 Published by Elsevier B.V. on behalf of Chinese Chemical Society and Institute of Materia Medica, Chinese Academy of Medical Sciences.

The metabolic disorder of uric acid (UA) in human body will lead to attacks of gout. Gout is a chronic inflammatory arthritis mainly caused by unhealthy dietary habits such as excessively regular intake of purine-rich foods including seafood and organ meats [1–3]. Purine-rich foods usually are metabolized into UA. When the metabolism of UA is disordered, UA will crystallize in the form of needle-like monosodium urate, precipitating and forming deposits of tophi in joints and in the surrounding tissues and result in the attack of gout [4]. With the growth in living standards, gout becomes more and more popular and affects about 1% and 2% of people's health in the western world [5,6]. Gout will lead to bone erosion and stone formation in the kidneys, and also result in subsequent urate nephropathy, or other complicated conditions such as lead poisoning, kidney failure, and death [7]. Gout is a chronic condition that requires lifelong monitoring and management. Because gout is closely linked to UA levels in the body, UA detection and monitoring are essential in the treatment of the disease.

Sweat-based UA detection devices have become more popular recently due to their ease of use compared to blood and urine-based UA detection devices, along with other advantages. Sweat contains abundant biological markers [8–11], and is easy to be collected and stored, enabling it to be an ideal analytical solution for UA measurement [12–16]. Previously reported sweat-based UA detection devices are usually constructed with two parts: detecting electrodes and substrates [17–19]. Electrochemical methods, such as enzymatic and non-enzymatic electrochemistry, are commonly used in the design of detecting electrodes for UA detection. While electrodes based on enzyme electrochemistry offer high selectivity [20–25], enzymes are prone to inactivation, which can reduce the reliability of the detection. Additionally, enzymes can be expensive, and fabrication processes for these electrodes are often complex [26,27]. As for electrodes based on non-enzyme and non-enzymatic electrochemistry [28–33], heavy metals such as Au [34,35], Co [36], Fe [37], and Ti [38] were used as catalysts during UA detection. However, these metals can be expensive and

* Corresponding authors.
E-mail addresses: wanjy@sjtu.edu.cn (J. Wan), jstao@scut.edu.cn (J. Tao).
[1] These authors contributed equally to this work.

https://doi.org/10.1016/j.cclet.2023.109103
1001-8417/© 2024 Published by Elsevier B.V. on behalf of Chinese Chemical Society and Institute of Materia Medica, Chinese Academy of Medical Sciences.

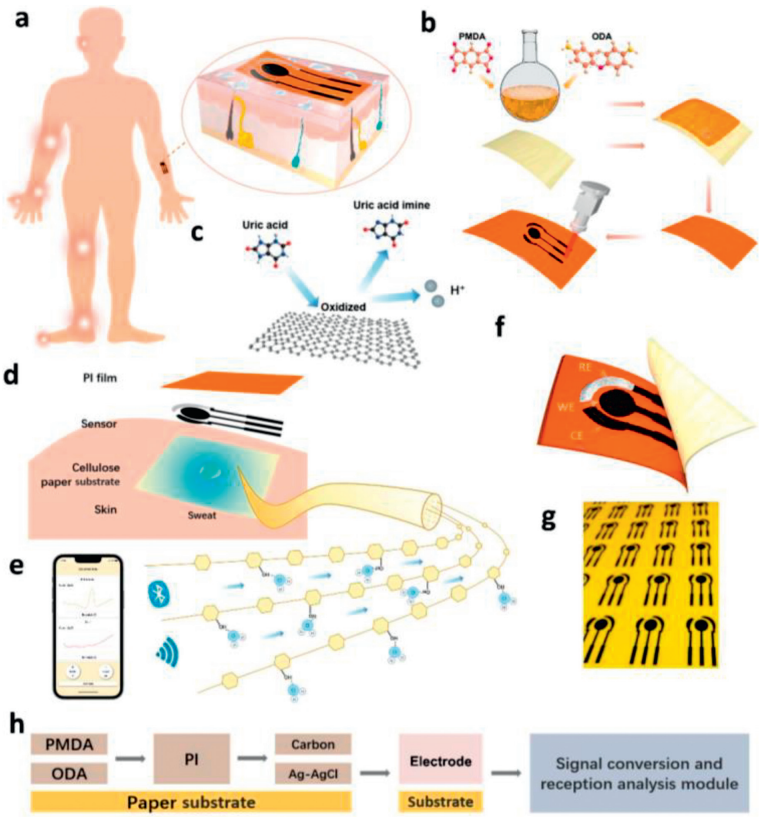

Fig. 1. Schematic diagram of the sensors of sweat UA detection. (a) Schematic diagram of the gout position in human body and the detection sensor. (b) Synthesis of polyimide (PI) films and fabrication of electrodes with laser engraving on PI films. The fabrication processes are simple and effective. (c) Mechanism of UA detection, uric acid is oxidized into uric acid imine on the surface of the electrodes. (d) Construction of the detection sensors with carbonized PI electrodes and cellulose paper substrates that can transport sweat initiatively. (e) The signal can be transmitted to mobile phones *via* Bluetooth. (f) Schematic diagram of the sensors with three electrodes. (g) Digital photographs of engraved sensor arrays, showing the sensors can be produced with high efficiency and low cost. (h) Illustration of the devices from raw materials preparation to sensor fabrication and device testing.

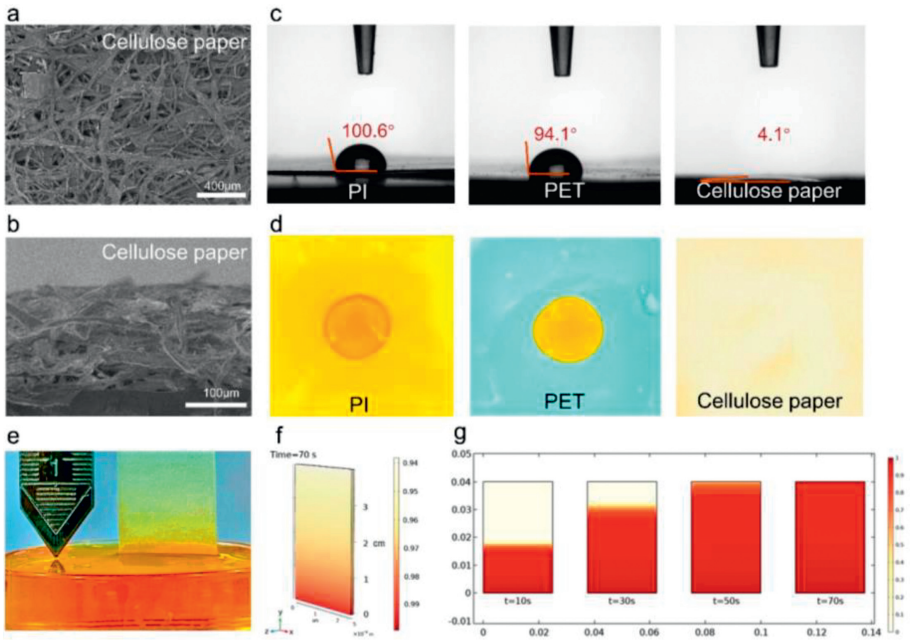

Fig. 2. Properties of cellulose paper substrates. (a) Surface and (b) cross-sectional SEM images of the cellulose paper substrates. (c) Digital photo images of the contact angles of PI, PET, and cellulose paper substrates. (d) Digital top view images of PI, PET, and cellulose paper substrates during contact angle tests. (e) Digital photo image of water absorption tests of cellulose paper substrates. (f, g) Simulation of the water absorption of cellulose paper substrates. The above results show cellulose paper substrates have standout hydrophilic properties.

may add to the overall cost of the device. For the substrates used in real-time UA detection, they are typically made of materials such as polyethylene terephthalate (PET) and polydimethylsiloxane [18,19,39]. While these substrates are readily available and highly flexible [40], they suffer from low hydrophilicity [41,42], which can adversely affect the performance of UA detection devices. In summary, the UA detection sensors reported in the literature are effective for detecting UA in sweat. However, the fabrication processes of the electrodes can be complex with some expensive materials used. Additionally, the hydrophobic nature of the substrates is a limiting factor, which may affect the performance and sensitivity of the device. Therefore, there is a need to develop simple, cost-effective, and highly hydrophilic sensors for UA detection.

Taking proper materials and processing methods may solve the challenge of UA detection sensors. Using simple and effective methods can greatly reduce costs [43–46]. As a simple and effective process, laser engraving has been introduced to selectively engrave an object recently [47,48]. Laser beams can deliver high energy to materials, causing them to heat up and prompt alterations to the material surface, such as direct chemical modifications, melting, or carbonization. This process can be used to laser-engrave materials such as wood, plastics, and metals [49]. Given its fast preparation speed and use of inexpensive raw materials, laser engraving is particularly well-suited for the mass production and application of materials. Polyimide (PI), known for its unique mechanical and chemical properties, is considered a valuable engineering plastic. Furthermore, it can be engraved using laser technology, making it a versatile material for a variety of applications. The high carbon content of PI, which contains repeating imide groups (-CO-N-OC-) and benzene rings [50], coupled with its unique aromatic structure, makes it easily laser-engravable. After laser engraving, PI can be carbonized into low-cost, high-performance sensors using its porous carbon structure [51–53], where laser-induced carbon on PI is a very popular strategy for synthesizing carbon-based electrodes. Cellulose paper, a natural and abundant material in our daily lives, is known for its lightweight, flexibility, porosity, and high hydrophilicity [54–57]. Due to the above advantages, it can be used as the substrates of UA detection sensors to collect, store, and pump sweat [58–64]. By combining PI and cellulose paper and utilizing laser engraving methods, it is possible to fabricate simple, low-cost, and highly hydrophilic sensors for detecting UA.

In this paper, we have developed a simple, low-cost, and highly hydrophilic sensor for sweat UA detection. The sensors were constructed with carbonized carbon electrodes and cellulose paper substrates. PI films were directly and effectively laser-engraved into porous carbon electrodes that have high specific area. Hydrophilic cellulose paper was used as substrate to collect, store, and transport sweat to the electrodes. UA was oxidated on the electrodes, and the concentration of UA is analyzed by measuring the oxidation reaction current. The properly constructed sensors exhibit high sensitivity and selectivity, low limit of detection, wide detection range, short response time, excellent reproducibility, and outstanding stability. We are confident that these newly developed sweat UA sensors hold great promise for the treatment of gout.

The design of the structure of the sensors is presented in Fig. 1. Usually, underexcretion of UA will deposit in the joints (Fig. 1a) in human body and form tophi that causes the attack of gout. The fabricated sensors can be attached to the surface of skin to monitor and detect UA in sweat (Fig. 1a). The sensors were constructed by carbon electrodes and cellulose paper substrates. The carbon electrodes were made by carbonized PI films through effective laser engraving methods (Fig. 1b). The PI-carbonized carbon electrodes could selectively catalyze the oxidation of UA at specific potentials (Fig. 1c). Meanwhile, sweat can be reserved and transported to the electrodes by the hydrophilic cellulose paper substrates because of the abundance of polar hydrogen groups on the surface of cellulose fibers (Fig. 1d). With the collected sweat, the UA can be monitored by the sensors, and the signal can be converted and transmitted to portal mobile terminals (Fig. 1e). The monitor electrodes consist of three electrodes, working electrode (WE), counter electrode (CE), and reference electrode (RE) (Fig. 1f). The sensors can be mass-produced with PI films aided with simple laser engraving methods, which significantly reduces the cost of the sensors (Fig. 1g). The main fabrication steps include raw materials preparation, sensor fabrication, and device testing (Fig. 1h).

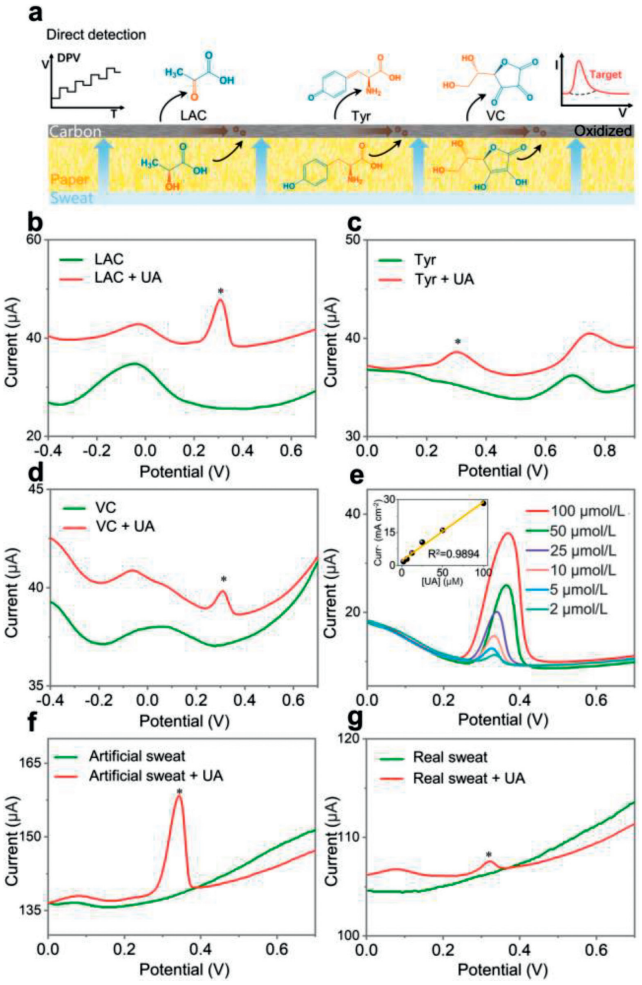

Fig. 3. Characterizations of the electrodes. (a) Schematics of direct detection of LAC, Tyr, and VC by the electrodes with DPV tests. Detection of UA in the presence of (b) LAC, (c) Tyr, and (d) VC, shows the electrodes have outstanding selectivity. (e) DPV tests of UA with different concentrations in 0.01 mol/L ABS solution, imply the electrodes have excellent sensitivity. UA can be detected with the electrodes both in (f) artificial sweat and (g) real human sweat.

Substrate has an important influence on the performance of sweat UA detection sensors. Ideal substrates for the sensors should have adequate sweat reservation and transportation ability. Thus, excellent hydrophilicity is essential for the substrates. Figs. 2a and b present the top and cross-section SEM images of cellulose paper substrates. From the top image, we can find many stacked cellulose fibers (Fig. 2a). With these fibers, the substrates exhibit a porous structure (Fig. 2b). Due to the abundance of hydrogen groups (-OH) on the surface of cellulose fibers, the substrates exhibit remarkable hydrophilicity (Figs. 2c and d). Compared with hydrophobic PI and PET substrates, the cellulose paper substrates

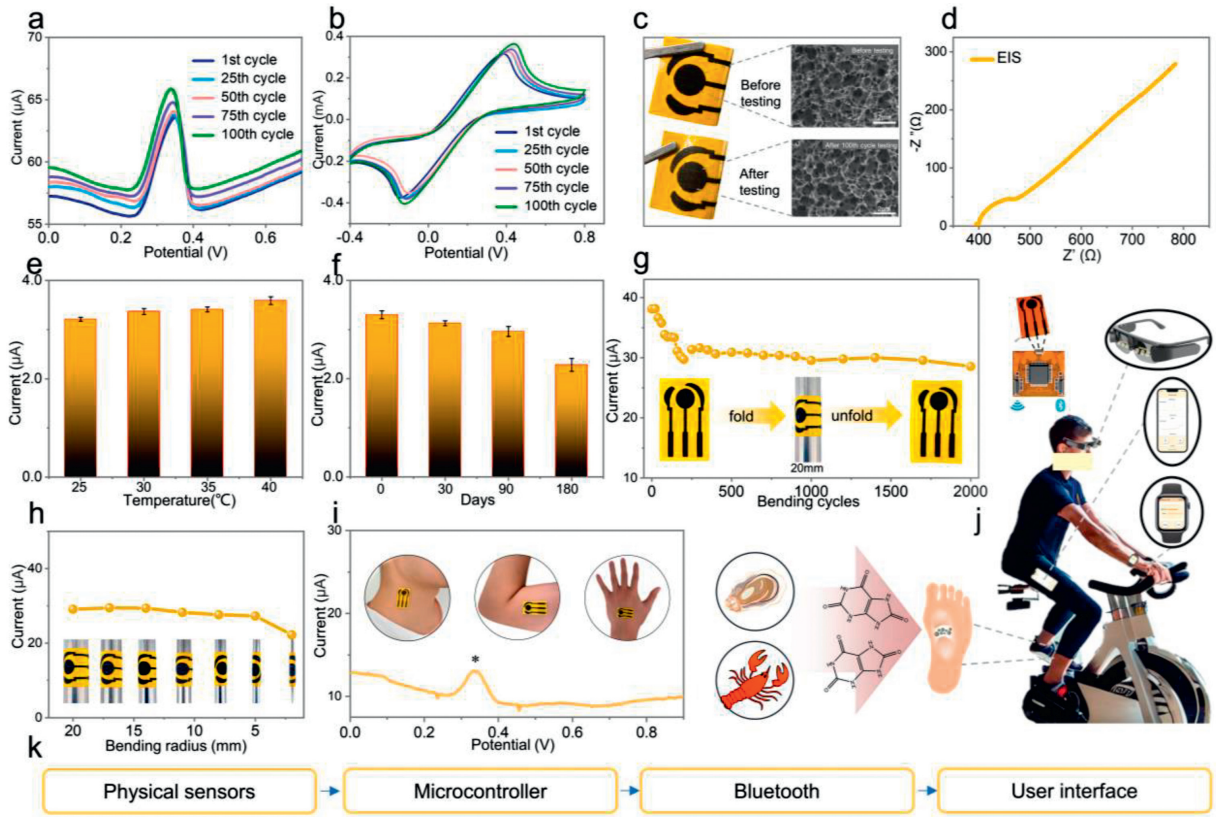

Fig. 4. Stability and flexibility tests of the electrodes. (a) Differential pulse voltammetry measurement of UA in 0.01 mol/L ABS with different testing cycles. (b) Different testing cycles of the cyclic voltammetry scans with the electrodes in 5 mmol/L $[Fe(CN)_6]^{3-}$ and 0.2 mol/L KCl solutions. (c) Digital photo images of the electrodes before and after 100 cycles of testing. Surface SEM images of the electrodes before and after 100 cycles of testing. (d) Electrochemical impedance spectroscopy tests were performed in solutions containing 5 mmol/L $[Fe(CN)_6]^{3-}$ and 0.2 mol/L KCl. (e) Effect of temperature on electrode sensitivity. (f) Effect of storage time on electrode sensitivity at room temperature. Effect of the electrodes of (g) different bending cycles and (h) bending radius on their sensitivity. (i) Schematic diagram of the wearable and flexible lab-on-skin patch attached to the different parts of human body. The curve is the detection of UA in artificial sweat on real human skin with DPV, which shows the sensors have good practicability. (j) Design of further UA testing lab. The intake of purine-rich food increases the risk of gout attacks. But the attacks can be effectively prognosticated, diagnosed, and treated by UA testing lab. The lab can be constructed with the sensors and the signal processing and transmitting module, and the testing results can be displayed with various mobile terminals. (k) Setup of the testing lab to wirelessly monitor UA.

exhibit the smallest contact angle (Fig. 2c) and the highest diffusion velocity (Fig. 2d). Fig. 2e presents the water absorption tests of cellulose paper substrates. A piece of cellulose paper with the size of 4 cm × 2.5 cm was dipped into water with red dye. And simulation was performed to analyze the water absorption and transportation ability with a simulation model of COMSOL Multiphysics 6.0 (Fig. 2f). The simulation results show cellulose paper substrates can be half-saturated in less than 30 s and can be fully saturated in 70 s (Fig. 2g). The results imply that the cellulose paper substrates have excellent hydrophilic ability. The excellent hydrophilic ability should be ascribed to the surface hydrogen groups of cellulose fibers and the abundant pores inside the substrate structure, which allows the capillary force effects to occur that are beneficial for the collection and transportation of sweat.

When conducting the selectivity and sensitivity characterization of the electrodes, we utilized the DPV (differential pulse voltammetry) method. DPV is a valuable electrochemical technique with high sensitivity, capable of carrying out direct analyses of electroactive molecules. Similar to UA, electroactive molecules such as lactic acid (LAC), tyrosine (Tyr) and vitamin C (VC) can be oxidized at specific potentials (Fig. 3a). Meanwhile, the concertation of electroactive molecules can be detected with the characteristic current peak. With these advantages, DPV can be used to do selectivity and sensitivity tests. Figs. 3b-g present the selectivity tests of UA at pH 4.7 which is close to the pH of human sweat. When LAC, Tyr, and VC were tested alone (green curves), only one peak can be observed in each figure that corresponds to the oxidation potential of LAC (−0.04 V, Fig. 3b), Tyr (0.7 V, Fig. 3c), and VC (0.1 V, Fig. 3d). When LAC, Tyr, and VC were tested together with UA (red curves), two distinctive peaks can be observed in each figure. One peak corresponds to the oxidation potential of LAC (−0.04 V, Fig. 3b), Tyr (0.7 V, Fig. 3c), and VC (0.1 V, Fig. 3d), and the other peak corresponds to the oxidation potential of UA that is about 0.3 V (Figs. 3b-d). The results show the electrodes have outstanding selectivity.

What is more, the sensitivity of the electrodes was also tested (Fig. 3e). The results show the electrodes can detect UA with a detection range from 2 μmol/L to 100 μmol/L. The sweat UA concentration of both ordinary individuals and patients with hyperuricemia-associated gout all falls into this range. The concentration of UA is directly proportional to the magnitude of the current, with an R^2 value of 0.9894 for the fitted regression line, showing the electrodes have excellent sensitivity in a wide detection range. Due to the absence of gout patients, we chose to use artificial sweat and sweat from healthy individuals as blank controls to perform tests. When UA was added in artificial sweat (Fig. 3f) and real human sweat (Fig. 3g), the obvious peaks of UA can be observed with the oxidation potential at 0.3 V, demonstrating the electrodes have excellent practicability.

To evaluate the stability and reproducibility of the sensor, we took the electrodes to carry out DPV measurements of the UA in 0.01 mol/L acetate-buffered saline (ABS) solution with different testing cycles from 0, 25, 50, 75 to 100. The oxidation peak potential of UA, as well as the detection sensitivity, remains stable (Fig. 4a). Meanwhile, we performed 100 cycles of cyclic voltammetry (CV) tests on the electrodes in 5 mmol/L $[Fe(CN)_6]^{3-}$, and the redox peaks almost remain stable (Fig. 4b). The DPV and CV testing results show the electrodes have excellent stability and reproducibility. Fig. 4c presents the digital photo images of the electrodes before and after 100-cycle testing, no obvious change can be observed on the surface of the electrodes. To further investigate the changes in the electrodes, we performed SEM tests. A three-dimensional porous structure can be observed from both images and no obvious collapse occurs after 100-cycle testing in the SEM images. Meanwhile, the porous structure also implies that the electrodes have high specific surface area and large contact area with analytes, which is beneficial for the detection sensitivity of the electrodes. What is more, we performed electrochemical impedance spectroscopy (EIS) tests on the electrodes and the results show they have excellent conductivity (Fig. 4d). Fig. 4e illustrates the impact of temperature on electrode sensitivity, revealing a slight increase in sensitivity as the temperature rises. Meanwhile, Fig. 4f demonstrates the effect of storage time on electrode sensitivity at room temperature, indicating a gradual decrease in sensitivity with increasing storage time. Figs. 4g and h present the effect of the electrodes with different bending cycles from 0 to 2000 and different bending radii from 2 mm to 20 mm on their sensitivity. The results indicate that detection sensitivity remains relatively stable, demonstrating that the electrodes exhibit exceptional flexibility, as well as outstanding mechanical and electrical stability.

The advantages presented by the detection sensors suggest the possibility of developing further UA testing scenarios and utilizing them to monitor the UA levels in the human body. During repetitive body movements, the flexible and hydrophilic nature of the cellulose-based substrate allows it to withstand friction and adhere to the body's surface after absorbing sweat. These sensors cannot only be attached to various locations on the skin's surface, but also, to assess practicality, we conducted detection tests for UA in artificial sweat (25 μmol/L UA) on real human skin (Fig. 4i). Because the UA concentration in normal human sweat is around 25 μmol/L, we opted for this concentration to create a more realistic simulation. According to the results, the sensors displayed outstanding sensitivity, as evidenced by the clear peak observed at around 0.3 V, which corresponds to the results in Figs. 3b–d. Furthermore, for the monitoring of gout induced by purine-rich food intake, in future research, it might be possible to integrate these sensors into a UA testing lab. We have proactively reserved three interfaces for the sensors in the integrated circuit, allowing for real-time display of sweat UA concentration levels on devices such as smart glasses, smartwatches, and mobile phones (Fig. 4j). With the aid of the process depicted in Fig. 4k, we envision our concept can be completely realized.

In conclusion, we have successfully developed a simple, low-cost, and hydrophilic sensor for sweat UA detection. The sensors were constructed by laser-engraved carbon electrodes and cellulose paper substrates. The laser-induced carbon electrodes boast high flexibility and a large specific surface area, while hydrophilic cellulose paper was employed as a substrate with high capability in collecting, storing, and transporting sweat. The developed sensors exhibit high sensitivity (0.4 μA L μmol^{-1} cm^{-2}) and high selectivity, wide linear range (2–100 μmol/L), short response time (10 s), excellent reproducibility and outstanding stability. Overall, the wearable sensors developed in this study exhibit significant potential as a promising and cost-effective strategy for the prognosis, diagnosis, and treatment of gout, as well as other metabolite disorders in the future.

Declaration of competing interest

The authors declare that they have no known competing financial interests or personal relationships that could have appeared to influence the work reported in this paper.

Acknowledgments

This work is funded by Guangdong Basic and Applied Basic Research Foundation (No. 2023A1515011388), Guangzhou City Industrial Science & Technology Projects (No. 202201010059), the fund from Guangxi China Tobacco Industry Co., Ltd. (No. 2022450000340057), the fund for the construction of Bengbu-SCUT Research Center for Advanced Manufacturing of Biomaterials (No. 20210190). The National Key Research and Development Program of China (No. 2018YFC1902102).

References

[1] C.F. Kuo, M.J. Grainge, W. Zhang, M. Doherty, Nat. Rev. Rheumatol. 11 (2015) 649–662.
[2] G. Ragab, M. Elshahaly, T. Bardin, J. Adv. Res. 8 (2017) 495–511.
[3] F. Perez-Ruiz, N. Dalbeth, T. Bardin, Adv. Ther. 32 (2015) 31–41.
[4] D. Lakshmi, M.J. Whitcombe, F. Davis, et al., Electroanalysis 23 (2011) 305–320.
[5] P. Richette, T. Bardin, Lancet 375 (2010) 318–328.
[6] N. Dalbeth, T.R. Merriman, L.K. Stamp, Lancet 388 (2016) 2039–2052.
[7] A. Abou-Elela, J. Adv. Res. 8 (2017) 513–527.
[8] T. Tat, G.R. Chen, X. Zhao, et al., ACS Nano 16 (2022) 13301–13313.
[9] L. Yin, M.Z. Cao, K.N. Kim, et al., Nat. Electron. 5 (2022) 694–705.
[10] Y.R. Yang, W. Gao, Chem. Soc. Rev. 48 (2019) 1465–1491.
[11] J.Q. Zhao, H.Y.Y. Nyein, L. Hou, et al., Adv. Mater. 33 (2021) 2006444.
[12] S. Emaminejad, W. Gao, E. Wu, et al., Proc. Natl. Acad. Sci. U. S. A. 114 (2017) 4625–4630.
[13] M. Bariya, H.Y.Y. Nyein, A. Javey, Nat. Electron. 1 (2018) 160–171.
[14] A.J. Bandodkar, W.J. Jeang, R. Ghaffari, J.A. Rogers, Annu. Rev. Anal. Chem. 12 (2019) 1–22.
[15] A. Koh, D. Kang, Y. Xue, et al., Sci. Transl. Med. 8 (2016) 366ra165.
[16] M. Chung, G. Fortunato, N. Radacsi, J. R. Soc. Interface 16 (2019) 20190217.
[17] L. Zhang, L. Wang, J. Li, et al., Nano Lett. 22 (2022) 5451–5458.
[18] X. Pei, M. Sun, J. Wang, et al., Small 18 (2022) 2205061.
[19] J. Xiao, Y. Luo, L. Su, et al., Anal. Chim. Acta 1208 (2022) 339843.
[20] Y.J. Lin, M. Bariya, H.Y.Y. Nyein, et al., Adv. Funct. Mater. 29 (2019) 1902521.
[21] D.F. Han, X.L. Li, Z.S. Liang, et al., Chin. Chem. Lett. 34 (2023) 107722.
[22] F. Qu, Z.W. Guo, D.F. Jiang, X.E. Zhao, Chin. Chem. Lett. 32 (2021) 3368–3371.
[23] G.L. Li, D. Wen, Chin. Chem. Lett. 32 (2021) 221–228.
[24] Q.Y. Chen, Y. Zhao, Y.Q. Liu, Chin. Chem. Lett. 32 (2021) 3705–3717.
[25] X. Xiao, eScience 2 (2022) 1–9.
[26] S. RoyChoudhury, Y. Umasankar, J. Jaller, et al., J. Electrochem. Soc. 165 (2018) B3168–B3175.
[27] M.Q. Yang, H. Wang, P. Liu, J. Cheng, Biosens. Bioelectron. 179 (2021) 113082.
[28] Y.F. Luo, M.R. Abidian, J.H. Ahn, et al., ACS Nano 17 (2023) 5211–5295.
[29] J.H. Li, L. Jiao, X. Xiao, et al., Electroanalysis 34 (2022) 1763–1771.
[30] J.R. Sempionatto, M.Y. Lin, L. Yin, et al., Nat. Biomed. Eng. 5 (2021) 737–748.
[31] J.R. Sempionatto, J.A. Lasalde-Ramirez, K. Mahato, et al., Nat. Rev. Chem. 6 (2022) 899–915.
[32] J.J. Zhang, L.L. Wang, Y. Xue, et al., Adv. Mater. 35 (2023) 2209324.
[33] K.K. Liu, Z. Meng, Y. Fang, H.L. Jiang, eScience 3 (2023) 100133.
[34] D.Z. Ji, Z.X. Liu, L. Liu, et al., Biosens. Bioelectron. 119 (2018) 55–62.
[35] F. Mazzara, B. Patella, G. Aiello, et al., Electrochim. Acta 388 (2021) 138652.
[36] F.X. Hu, T. Hu, S.H. Chen, et al., Nano Micro Lett. 13 (2021) 7.
[37] E. Sohouli, E.M. Khosrowshahi, P. Radi, et al., J. Electroanal. Chem. 877 (2020) 114503.
[38] N. Murugan, R. Jerome, M. Preethika, et al., J. Mater. Sci. Technol. 72 (2021) 122–131.
[39] Y.R. Yang, Y. Song, X.J. Bo, et al., Nat. Biotechnol. 38 (2020) 217–224.
[40] S.Y. Huang, Y. Liu, Y. Zhao, et al., Adv. Funct. Mater. 29 (2019) 1805924.
[41] G. Li, Z.G. Qiu, Y. Wang, et al., ACS Appl. Mater. Interfaces 11 (2019) 10373–10379.
[42] Z.X. Wu, H.J. Ding, K. Tao, et al., ACS Appl. Mater. Interfaces 13 (2021) 21854–21864.
[43] X.S. Hu, D.X. Zuo, S.R. Cheng, et al., Chem. Soc. Rev. 52 (2023) 1103–1128.
[44] C. Li, Z.Y. Liang, Z.Z. Li, et al., Nano Lett. 23 (2023) 4014–4022.
[45] Y.C. Yin, C. Li, X.S. Hu, et al., ACS Energy Lett. 8 (2023) 3005–3012.
[46] D. Zuo, L. Yang, Z. Zou, et al., Adv. Energy Mater. (2023), doi:10.1002/aenm.202301540.
[47] M.Q. Wang, Y.R. Yang, J.H. Min, et al., Nat. Biomed. Eng. 6 (2022) 1225–1235.
[48] M.Q. Wang, Y.R. Yang, W. Gao, Trends Chem. 3 (2021) 969–981.

[49] J. Lin, Z. Peng, Y. Liu, et al., Nat. Commun. 5 (2014) 5714.
[50] K. Vanherck, G. Koeckelberghs, I.F.J. Vankelecom, Prog. Polym. Sci. 38 (2013) 874–896.
[51] A. Kothuru, C.H. Rao, S.B. Puneeth, et al., IEEE Sens. J. 20 (2020) 7392–7399.
[52] M. Abdulhafez, G.N. Tomaraei, M. Bedewy, ACS Appl. Nano Mater. 4 (2021) 2973–2986.
[53] E.R. Mamleyev, S. Heissler, A. Nefedov, et al., npj Flex. Electron. 3 (2019) 2.
[54] X.Z. Wang, Z.Q. Pang, C.J. Chen, et al., Adv. Funct. Mater. 30 (2020) 1910417.
[55] B. Jiang, C.J. Chen, Z.Q. Liang, et al., Adv. Funct. Mater. 30 (2020) 1906307.
[56] M.W. Zhu, Y.L. Wang, S.Z. Zhu, et al., Adv. Mater. 29 (2017) 1606284.
[57] H. Pan, G.R. Chen, Y.M. Chen, et al., Biosens. Bioelectron. 222 (2023) 114999.
[58] W. Dungchai, O. Chailapakul, C.S. Henry, Anal. Chem. 81 (2009) 5821–5826.
[59] J.L. Osborn, B. Lutz, E. Fu, et al., Lab Chip 10 (2010) 2659–2665.
[60] W. Dungchai, O. Chailapakul, C.S. Henry, Analyst 136 (2011) 77–82.
[61] R. Fobel, A.E. Kirby, A.H.C. Ng, et al., Adv. Mater. 26 (2014) 2838–2843.
[62] M.M. Hamedi, A. Ainla, F. Guder, et al., Adv. Mater. 28 (2016) 5054–5063.
[63] A. Nilghaz, L.Y. Guan, W.R. Tan, W. Shen, ACS Sens. 1 (2016) 1382–1393.
[64] K. Yamada, H. Shibata, K. Suzuki, D. Citterio, Lab Chip 17 (2017) 1206–1249.